frontiers | Frontiers in Earth Science

TYPE Original Research
PUBLISHED 14 July 2023
DOI 10.3389/feart.2023.1229851

OPEN ACCESS

EDITED BY
Yong Wang,
Southwest Petroleum University, China

REVIEWED BY
Dan Ma,
China University of Mining and Technology, China
Simone Mineo,
University of Catania, Italy
Yanlin Zhao,
Hunan University of Science and Technology, China
Ruyue Wang,
SINOPEC Petroleum Exploration and Production Research Institute, China

*CORRESPONDENCE
Xiaofei Fu,
fuxiaofei2008@sohu.com

RECEIVED 27 May 2023
ACCEPTED 06 July 2023
PUBLISHED 14 July 2023

CITATION
Jia R, Fu X, Jin Y, Wu T, Wang S and Cheng H (2023), Mechanical properties of mudstone caprock and influencing factors: implications for evaluation of caprock integrity.
Front. Earth Sci. 11:1229851.
doi: 10.3389/feart.2023.1229851

Mechanical properties of mudstone caprock and influencing factors: implications for evaluation of caprock integrity

Ru Jia[1,2,3], Xiaofei Fu[1,2,3]*, Yejun Jin[1,2,3], Tong Wu[1,2,3], Sheng Wang[1,2,3] and Huijie Cheng[4]

[1]Key Laboratory of Continental Shale Hydrocarbon Accumulation and Efficient Development, Ministry of Education, Northeast Petroleum University, Daqing, Heilongjiang, China, [2]Sanya Offshore Oil and Gas Research Insitute, Northeast Petroleum University, Sanya, Hainan, China, [3]Institute of Unconventional Oil and Gas, Northeast Petroleum University, Daqing, Heilongjiang, China, [4]Daqing Yusulin Oilfield Development Co., Ltd., Daqing, Heilongjiang, China

Mudstone is the most common cap rock in petroliferous basins. The mechanical properties of mudstone in different areas and buried depths are obviously different, which directly affects the brittleness and ductileness of caprock and its deformation characteristic. This research carried out X ray diffraction (XRD) rock mineral composition analysis, microscopic observation of mineral structural characteristics and rock mechanics triaxial compression tests under different conditions on six groups of mudstone samples from three basins. On this basis, establish numerical model to simulate the fracture deformation of mudstone under geological conditions, and to clarify the influence of different factors on the rock mechanics of mudstone. Compare and analyze the fracture characteristics and stress-strain curves of mudstone samples after the test show that, the confining pressure is the most direct factor affecting the mechanical properties and deformation mechanism of mudstone in the range of oil and gas enrichment depth. Although the formation temperature has a certain influence on the rock deformation, the effect is very limited, and it is difficult to have an essential influence on the rock deformation without the action of confining pressure. The mineral composition of mudstone is also one of the main factors affecting the mechanical deformation of rock. The comparison between the content of main minerals and the mechanical parameters of rock shows that the mechanical properties of rock and the transformation of brittleness and ductileness of mudstone have the most obvious correlation with clay minerals. Numerical simulations show that, pore fluid pressure is an important factor that cannot be ignored in overpressured caprocks. Higher pore fluid pressure can significantly inhibit the transition process of rock brittleness and ductileness, and at the same time affect the fracture mode of mudstone, which is of great significance for the evaluation of caprock integrity.

KEYWORDS

mudstone, caprock, rock mechanic, confining pressure, brittle and ductile, fracture

1 Introduction

Mudstone is the most common type of sedimentary rock, which refers to the fine-grained sedimentary rock composed of more than 50% particles with particle size less than 0.0039 mm, including silty mudstone, calcareous mudstone, etc. The composition of mudstones is often very complex, usually composed of clay minerals (kaolinite, illite, montmorillonite, chlorite, etc.), clastic minerals (quartz, feldspar, mica, etc.) and some authigenic non-clay minerals (Fe and Mn oxides and carbonate minerals, etc.). The characteristics of high clay mineral content and fine grained deposition make mudstones often have low porosity and permeability, and make them an effective cover for udnerground oil and gas enrichment. Mudstone is the most common caprock of large and medium-sized oil and gas fields in the world (Grunau, 1987; Lv et al., 1996; Ovcharenko et al., 2007; Fu et al., 2008; Fu et al., 2018), and in terms of capped reserves, mudstone caprock has the largest recoverable oil and gas reserves.

Mechanistically, the reason why mudstone can seal such abundant oil and gas is due to its low physical properties and high capillary pressure. However, in the unsuccessful trap of oilfield exploration and discovery due to preservation conditions, some mudstones still have high capillary pressure and sealing ability, but failed to accumulation, which means that the physical sealing ability of mudstones may not be the key to affect reservoir preservation conditions (Downey, 1984; Fu et al., 2018; Faerseth et al., 2007; Mildren et al., 2005), but whether the caprock fractured and the degree of fracturing are the key factors that restrict whether the oil and gas can be sealed. However, due to the different mineral composition and diagenetic evolution degree of mudstone in different regions, as well as the constant change of geological conditions such as stratum temperature, pressure and fluid properties, rock mechanical properties of mudstone are significantly different (Handin et al., 1963; Dewhurst et al., 2002; Brantut et al., 2011; Li et al., 2016; Zhao et al., 2019; Chen et al., 2020; Wu, 2020; Zhao et al., 2020; Yu et al., 2021; Zhao et al., 2021; Ma et al., 2022; Ma et al., 2023; Fuenkajorn et al., 2012). Previous studies have shown that mudstone will gradually transform from brittle fracture to ductile deformation with the increasing temperature and confining pressure in the formation (Figure 1) (Paterson, 1958; Wu, 2020; Lu et al., 2021), and the fracture characteristics of mudstone are different in different stages of brittle and ductile, which directly leads to the need to use different methods to evaluate the integrity and effectiveness of the cap layers. For the evaluation of the brittle and ductile stage of the mudstone caprock, scholars have proposed a variety of determination methods, such as dension-strain (Corcoran and Dore, 2002; Jin et al., 2013), BRI and OCR (Ingram et al., 1997; Ingram and Urai, 1999; Nygård et al., 2006), and rock fracture criteria (Fu et al., 2015; Wang et al., 2019; Wu, 2020) and energy conservation method (Wang, 2021). Corcoran and Dore. (2002) used density and stress variables during fracture to quantitatively determine the brittle and ductile transformation process of mudstone and shale, and believe that the density of mudstone and shale in the brittle stage is greater than 2.5 g/cm^3, and the strain before fracture is less than 3%. The density of mudstone and shale in the ductile stage is less than 2.25 g/cm^3, and the strain before fracture is more than 8%. The density between them is in the brittle and ductile stage. Ingram et al. (1997) proposed to use the over-consolidation ratio (OCR) to quantitatively determine the occurrence of caprock fracture, and believed that when the OCR was greater than 2.5, the caprock was brittle and the risk of leakage was increased (Ingram and Urai, 1999; Nygård et al., 2006). The

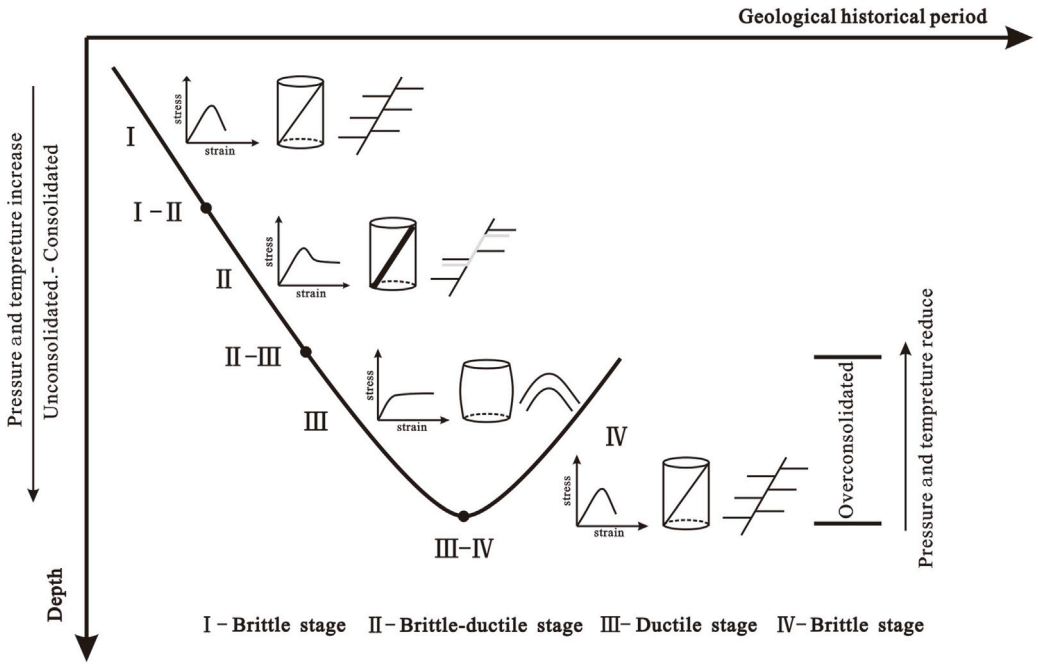

FIGURE 1
Burial history and brittle-ductile evolution model of mudstone.

Mohr-Coulomb fracture criterion, Byerlee friction law and Goetze criterion were used by Fu et al. (2015) to quantitatively identify the critical confining pressure of rock brittle-ductile transition (Wang et al., 2019; Wu et al., 2022). Based on the principle of energy conservation after the peak, Wang (2021) proposed the brittleness index, which can determine the brittleness degree of rocks. The above methods are almost all based on rock mechanical parameters, however, due to the scarcity of mudstone cap samples, systematic triaxial stress tests with different temperature, pressure and pore fluid pressure are rarely carried out with underground mudstone samples. Although there are researches on the mechanical properties of mudstone, there are still few researches on the influencing factors leading to its change, which affects the study on the brittle and ductile transformation and fracture law of mudstone cap, and restricts the development of research on the sealing and integrity of mudstone caprock.

In this paper, mudstone samples from several basins are selected to carry out triaxial mechanical compression tests under different conditions. Based on experimental data and numerical simulation, the influences of various factors on rock mechanics and brittle-ductile deformation of mudstone are discussed. It is hoped that the results of this study can provide some reference for the evaluation of brittle and ductile of caprock layer. In order to provide certain support for further research on the integrity of mudstone caprock.

2 Sample and method

2.1 Sample source

Samples used in this study are derived from three basins. The firsst group sample come from Tugulu Group Formation in the southern margin of the Junggar Basin. The second group sample come from the Jidike Formation of the Dongqiu anticline of the Kuche Depression in the Tarim Basin. Both groups of samples were taken from outcrop areas. The Junggar Basin and Tarim Basin are located on the north and south sides of the Tianshan Mountains in Xinjiang. They are both superimposed foreland basins that have undergone multiple tectonic evolution and contain a lot of oil and gas resources with a long history of exploration. There are several reservoir-caprock assemblages in the southern margin of Junggar Basin, among which the mudstone of the Lower Cretaceous Tugulu Group is the main caprock layer with large sedimentary thickness and stable regional distribution (Tian et al., 2017). The Kuqa Depression is located in the northof Tarim Basin, the Dongqiu anticline is a second-order structural belt in the southern margin of Kuqa Depression (Fu et al., 2015; Wang et al., 2019; Wu et al., 2022). The Jidike Formation is a set of regional caprock layer of this structure belt, which provides favorable conditions for oil and gas accumulation. The third and fourth groups of samples were taken from mudstone of Neogene Huangliu Formation in Dongfang and Ledong areas of Yinggehai Basin. It is a direct sample from the drilling core. The Yinggehai Basin is a typical Cenozoic sedimentary basin on the northwestern continental shelf of the northern South China Sea (Xie, 2009; Xie et al., 2012). Dongfang and Ledong area are located in the central depression zone of the basin. The Huangliu Formation is the most stable and extensive regional caprock layer in the basin, and the natural gas is mainly enriched under this cap layer (Jia et al., 2021).

The field samples have not undergone large-scale weathering, the core samples are kept intact, and all the samples had no natural fracture developed.

2.2 Sample preparation

This study involves X-ray diffraction analysis of rock and mineral composition, microscopic observation of rock and mineral microstructure and rock mechanics triaxial compression experiment. The sampels of X-ray diffraction analys is powder, and the rock sample to be measured needs to be crushed to 200 mesh powder samples. Microscope observation requires the rock sample to be made into a standard slices for observation, with a sample thickness of about 0.03 mm. Rock mechanics triaxial compression test samples need to be machined into cylinders. In addition, in order to avoid mudstone expansion in contact with water or breakage during the drilling process, the samples were processed by wire cutting. In the sample preparation process, large field samples or drilling core samples are first placed on the diamond wire cutting device, the instrument model is SSP-505. The diamond powder distribution on the surface of the wire is fine and uniform, there is no local accumulation phenomenon, and the surface of the prepared sample is flat and smooth. The device can be automatically operated by numerical control throughout the whole process. The diamond cutting line works in multiple ways according to the set sample shape, and finally prepared into a cylindrical body with a diameter of about 25 mm and a height of about 50 mm.

2.3 Experimental equipment

X-ray diffraction analysis of rock and mineral composition is performed using the D8AA25 model X-ray diffractometer of Bruker, Germany, which requires the powder sample to be placed in the sample bin for X-ray scanning. Maximum output power of X-ray generator is 3.0 kW, using international standard size ceramic X-ray tube, target Cu, The accuracy of goniometer measurement was better than 0.01°, according to the latest standard SY/T5163-2018. Mineral structural characteristics of rock were observed using Leica DM4 polarizing microscope.

The triaxial compression experiment in this study was completed by the RTR-2000 high-pressure rock triaxial dynamic test system of GCTS (Figure 2), which is mainly used to test rock physical parameters under different temperature, pressure and pore fluid pressure conditions. The equipment is equipped with high stiffness loading frame with load stiffness up to 10 M N/mm; it can provide maximum axial pressure of 200 0 kN, maximum confining pressure of 140 MPa, maximum pore fluid pressure of 140 MPa, maximum temperature of 200°C, and fluid displacement rate of 0.001 cc–2.0 cc/min, deformation rate was 0.03 mm/min. A constant temperature during the test can be achieved through the heating element on the device. Before the test, a thin polyolefin heat shrinkable pipe whose length is longer than the cylindrical sample should be used. After covering the piston on the top and bottom, it can be sealed by heating the pipe by usinig a heat gun from the

FIGURE 2
RTR-2000 high pressure rock triaxial dynamic test system.

bottom and top to isolate the sample and hydraulic oil, which can avoid affecting the test results. The change of test conditions and data acquisition during the test can be completely controlled and recorded by computer. The axial load, deviational stress, confining pressure, axial strain, radial strain and volumetric strain are recorded at a time interval of 2s. The test accuracy and data collection and analysis methods meet all the requirements of "GB/T 50266-2013 Standard for test methods of engineering rock mass" and the methods suggested by ISRM of the International Society of Rock Mechanics.

2.4 Experimental scheme of triaxial compression test

The main purpose of this experiment is to explore the fracture characteristics of mudstone under different geological conditions and the influence of geological factors on the mechanical properties and deformation characteristics of mudstone. Therefore, six groups of experiments were carried out successively, each group of experiments with only a single factor as a variable, to obtain the stress-strain curve and mechanical characteristic parameters of mudstone samples under different test conditions. In other words, in the same group of tests, only one parameter of the three parameters of temperature, confining pressure and pore fluid pressure is changed, and the other two parameters are fixed. The specific setting of experiment parameters is based on the source basin of the samples, in which the corresponding layer of the Junggar and Tarim Basin samples are shallowly buried, with little temperature change and low fluid pressure, so influence of the confining pressure on the mudstone deformation is mainly considered. Samples from Dongfang and Ledong areas of Yinggehai Basin are deeply buried, taken from 2,994 to 3,634 m respectively. Within this depth range, the formation develops abnormally high fluid pressure and temperature (Li et al., 2022), the formation pressure coefficient is 1.5–2.2, and the temperature gradient is 37–50°C/km. Parameters in the experiment were set to simulate changes in real geological conditions as much as possible. The temperature setting range is 25–160°C, the confing pressure range is 15–110 MPa, and the pore fluid pressure range is 5–55 MPa, as shown in Table 1.

3 Results

3.1 Mineral composition and microstructure characteristics of the samples

X-ray diffractometer tests show that the mineral composition of mudstone samples is mainly composed of clay minerals (24.3%–33.8%), quartz (20.7%–42.2%), feldspar (12.1%–18.7%), dolomite (2.0%–5.5%), ankerite (about 15%), calcite (10.0%–16.6%) and other minerals (1.8%–10.0%) (Table 2).

Microscopic observations show that the samples are mainly argillaceous and supported by typical matrix supporting. The quartz particles were small in size, ranging from 2.7 to 47.5 μm, and were mainly mud and silty, dispersed among clay minerals. Most of the particles in the matrix were not in contact with each other but were distributed in floating isolation (Figure 3). The whole sample is mainly in massive structure, no obvious stratification or lamination structure is developed, and no micro-cracks are found under the microscope.

3.2 Results of the triaxial compression test of rock mechanics

3.2.1 Samples from Junggar Basin

In the first group of experiments, the mudstone samples of Tugulu Group in the southern margin of Junggar Basin showed

TABLE 1 Parameter setting of triaxial compression experiment of mudstone samples.

Sample Source	Group	No.	Diameter	Length	Density	Confining Pressure	Temperature	Pore fluid Pressure	Cohesion	Internal friction angle	Coefficient of internal friction	Young modulus	Poisson's ratio	Peak strength	Residual strength
			(mm)	(mm)	(g/cm^3)	(MPa)	(°C)	(MPa)	(MPa)	(°)	—	(GPa)	—	(MPa)	(MPa)
The Tugulu Group Formation in the southern margin of the Junggar Basin	1	M1	24.92	49.28	2.48	5.00	25.00	0.00	21	40.22	0.85	9.65	0.18	62.1	8.9
		M2	24.48	51.27	2.48	10.00	25.00	0.00				12.81	0.21	141.7	85.6
		M3	24.88	50.01	2.48	20.00	25.00	0.00				12.50	0.22	150.5	96.5
		M4	24.57	52.43	2.48	40.00	25.00	0.00				17.43	0.24	225.3	153.5
		M6	24.94	48.43	2.48	60.00	25.00	0.00				15.98	0.24	249.2	176
		M7	24.96	49.95	2.48	75.00	25.00	0.00				17.71	0.28	299.6	195
		M8	24.92	49.28	2.48	90.00	25.00	0.00				16.84	0.28	306.8	252
		M9	24.72	49.53	2.48	110.00	25.00	0.00				17.78	0.29	368.4	273
The Jidike Formation in Dongqiu anticline of the Kuche Depression in the Tarim Basin	2	J1	24.86	52.33	2.48	5.00	25.00	0.00	8.7	42.7	0.92	7.91	0.18	54.55	5.79
		J2	25.17	52.11	2.48	10.00	25.00	0.00				13.24	0.22	106.78	57.97
		J3	25.22	51.97	2.48	20.00	25.00	0.00				11.58	0.25	125.3	82.85
		J4	25.18	52.78	2.49	40.00	25.00	0.00				15.34	0.23	196.74	119.89
		J5	25.16	51.85	2.48	65.00	25.00	0.00				21.00	0.27	197.1	177.5
The Huangliu Formation in Ledong Area of the Yinggehai Basin	3	L1	24.99	50.23	2.69	15.00	150.00	0.00	17	23.09	0.42	10.72	0.19	59.5	21.3
		L2	24.92	51.04	2.7	25.00	150.00	0.00				17.64	0.17	88.6	52.2
		L3	24.74	50.66	2.7	40.00	150.00	0.00				9.24	0.2	95.8	66.1
		L4	24.72	49.72	2.7	55.00	150.00	0.00				11.73	0.18	137	122
		L5	24.76	51.3	2.7	75.00	150.00	0.00				12.56	0.21	146.4	152.6
		L6	24.88	51.75	2.69	95.00	150.00	0.00				11.97	0.22	158.5	155.6
		L7	24.81	49.28	2.7	110.00	150.00	0.00				15.85	0.18	163.7	193.2
The Huangliu Formation in Dongfang Area of the	4	H1	24.95	50.13	2.67	60.00	130.00	55.00	21.3	23.6	0.44	14.59	0.18	69.3	27.3
		H2	24.92	51.01	2.66	70.00	130.00	55.00				15.28	0.19	88.3	53.7
		H3	24.9	50.3	2.67	80.00	130.00	55.00				12.67	0.23	101.5	67.4

(Continued on following page)

10.3389/feart.2023.1229851

TABLE 1 (*Continued*) Parameter setting of triaxial compression experiment of mudstone samples.

Sample Source	Group	No.	Diameter	Length	Density	Confining Pressure	Temperature	Pore fluid Pressure	Cohesion	Internal friction angle	Coefficient of internal friction	Young modulus	Poisson's ratio	Peak strength	Residual strength
			(mm)	(mm)	(g/cm^3)	(MPa)	(°C)	(MPa)	(MPa)	(°)	—	(GPa)	—	(MPa)	(MPa)
Yinggehai Basin		H4	24.94	49.33	2.68	95.00	130.00	55.00				13.54	0.22	115.8	100.9
		H5	25.1	49.94	2.66	110.00	130.00	55.00				16.45	0.2	139.3	132.2
	5	H6	24.73	48.46	2.67	80.00	25.00	55.00				17.40	0.29	129.5	92.4
		H7	24.58	50.59	2.68	80.00	50.00	55.00				11.87	0.27	118.3	72.9
		H8	24.67	51.75	2.68	80.00	100.00	55.00				13.76	0.28	109.5	65.4
		H9	24.58	48.76	2.70	80.00	160.00	55.00				14.89	0.22	100.2	68.5
	6	H10	24.48	49.56	2.69	80.00	130.00	5.00				12.24	0.18	158.9	154.4
		H11	25.18	51.58	2.68	80.00	130.00	15.00				18.67	0.22	160.9	154.8
		H12	24.33	50.98	2.69	80.00	130.00	35.00				13.58	0.24	143.8	118.3
		H13	25.18	48.56	2.68	80.00	130.00	45.00				14.13	0.23	134.9	93.1

10.3389/feart.2023.1229851

10.3389/feart.2023.1229851

TABLE 2 Mineral composition and relative content of mudstone samples.

Sample	Quartz	Potassium feldspar	Anorthose (%)	Calcite	Dolomite (%)	Ankerite (%)	Hematite (%)	Siderite (%)	Pyrite	Analcite (%)	Gypsum	Clay minerals
Source	(%)	(%)		(%)					(%)		(%)	(%)
The Tugulu Group Formation in the southern margin of the Junggar Basin	20.7	3.7	15.0	11.3		15.0	1.9			6.4	1.7	24.3
The Jidike Formation in Dongqiu anticline of the Kuche Depression in the Tarim Basin	27.9		15.4	16.6	5.5					3.1		31.5
The Huangliu Formation in Dongfang Area of the Yinggehai Basin	35.1	1.3	10.8	15.2	2.0			0.6	1.2			33.8
The Huangliu Formation in Ledong Area of the Yinggehai Basin	42.2	2.2	11.9	10.0				1.8				31.9

obvious fracture after triaxial compression (Figure 4A). The tensional fracture developed under the condition of confining pressure less than 10 MPa, and an obvious "axial spliting" phenomenon can be seen on the sample (Basu et al., 2013), the "snap" can be heard during the experiment. When the confining pressure exceeds 10 MPa, the mudstone began to shear fracture. It can be seen from the macroscopic fracture characteristics of the samples that the fracture strain of rocks are relatively concentrated under the confining pressure of 20–110 MPa. The sample developed a non-cohesive primary shear fracture and some smaller secondary fractures. The Angle between the primary shear fracture and compressive stress increased with the increase of confining pressure, but the whole sample still showed typical brittle deformation characteristics. The morphology of stress-strain curve shows that under low confining pressure, elastic deformation mainly occurs before the mudstone reaches the peak strength, but suddenly drops after the peak strength, and has a large stress drop (the difference between peak strength and residual strength). In the medium confining pressure condition, the mudstone first occurs elastic deformation, and then a small ductile deformation stage. When the strain hardening reaches the peak strength of the sample to a certain extent, he curve suddenly drops, but also has a large stress drop. Under high confining pressure conditions, the stress-strain curve characteristics are similar, but the duration of ductile deformation increases obviously (Figure 5A).

3.3 Samples from Tarim Basin

The second group of experiments used mudstone samples from the Jidike Formation of the Dongqiu anticline in the Kuqa Depression, Tarim Basin. Under the confining pressure of 5 MPa, it is similar to the first group of experiments, with obvious tensional fracture (Figure 4B) and small residual strength (Figure 5B). When the confining pressure reaches 10 MPa, shear fractures are developed and the shear Angle is less than 30°. When the confining pressure is 20 and 40 MPa, the shear Angle is close to 30°, resulting in the whole rock sample being penetrated. When the confining pressure is 65 MPa, there is still a some stress drop, but there is no obvious penetration fracture on the surface of the mudstone sample, and only some small conjugate shear fractures still exist. The peak strength of the stress-strain curve increases with the increase of confining pressure, and the curve drops rapidly after reaching the peak strength under low confining pressure. With the increase of confining pressure, mudstone gradually shows the characteristics of ductile deformation after reaching the peak strength, and the stress-strain curve tends to be flattened. The sample with 40 MPa confining pressure fractured when the axial strain reached 2%. The curve shape of the 65 MPa confining pressure sample decreased after compression, but the stress drop was significantly reduced. It can be inferred that the mudstone was in the transition stage from brittle stage to brittle-ductile stage.

3.4 Samples from Yinggehai Basin

The third group of experiments is mudstone in Ledong area of Yinggehai Basin. The shear fractures are mainly penetrated the

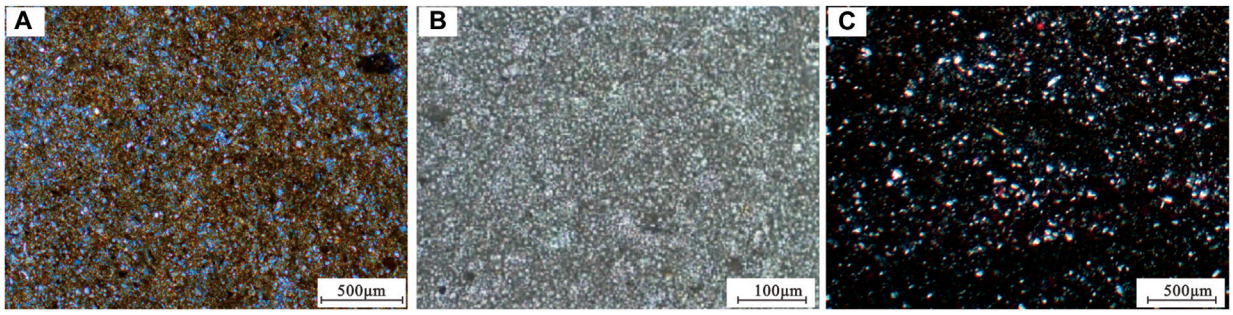

FIGURE 3
The microstructure characteristics of the samples, **(A)** the sample come from the Jidike Formation of the Dongqiu anticline of the Kuche Depression in the Tarim Basin; **(B)** the sample come from Tugulu Group Formation in the southern margin of the Junggar Basin (Tian et al., 2017), **(C)** the sample come from the Huangliu Formation of the Yinggehai Basin.

samples under confining pressure of 15–55 MPa (Figure 4C). When the confining pressure reaches a certain degree, there is no obvious fracture on the surface of the sample and ductile expansion occurs locally. Under the confining pressure condition of 15 MPa, the stress-strain curve showed obvious brittle deformation characteristics with significant stress drop, corresponding to a peak intensity of 59.46 MPa, when the confining pressure increases to 55 MPa, the stress-strain curve is characterized by ductile deformation. After the curve reaches the peak intensity, no obvious stress drop can be observed in the curve, and it gradually become flat (Figure 5C). The samples from the fourth to the sixth groups were all from Dongfang area of the Yinggehai Basin, and the samples showed similar deformation characteristics to the first three samples. Under the condition of low confining pressure, the rock shows obvious brittle fracture (Figure 4D). With the increase of effective confining pressure, the rock gradually shows ductile deformation characteristics. When the confining pressure is 80 MPa and the pore fluid pressure is 55 MPa, that is, the effective confining pressure is 25 MPa, the stress-strain curve is characterized by brittle fracture, with obvious stress drop. However, when the confining pressure is 95 MPa and the pore fluid pressure is 55 MPa, that is, the effective confining pressure is 40 MPa, The stress - strain curves show the characteristics of ductile deformation (Figure 5D).

Although the sources of the above test mudstone samples are different, the fracture characteristics and stress-strain curve morphology of the compressed samples are generally similar, that is, under the condition of low confining pressure, tensile fracture and shear fracture occur after the compression of the rocks, and obvious penetrated fracture occurs on the sample. With the gradual increase of confining pressure, the fracture scale on the sample decreases, resulting in conjugate fracture, and gradually shows the ductile characteristic of local expansion. The stress-strain curve also changes obviously with the increase of confining pressure, and the peak strength and corresponding strain increase gradually. In the brittle stage of low confining pressure, the stress-strain curve drops rapidly after reaching the peak strength, showing a large stress drop. With the increase of confining pressure, the stress drop gradually decreases. When the mudstone reaches the ductile deformation, the stress drop is close to 0, and no obvious drop after the stress-strain curve reaches the peak strength.

4 Discussion

4.1 The influence of different factors on the mechanical properties of mudstones

The rock mechanical properties of mudstone are influenced by various geological factors, but different factors can affect them differently. The mudstone samples from three basins and four regions were selected to mainly discuss the influence of temperature, confining pressure, pore fluid pressure and rock mineral components on the mechanical properties of mudstone rocks. Although the number of samples in this experiment is limited, which makes the research results have some limitations to some extent, some regularity can still be found in the limited experimental results, hoping to provide some basis for future research.

4.1.1 Temperature

Many scholars have confirmed that increasing temperature can effectively promote the ductile deformation of rock (Heuze, 1983; Gao et al., 2005; Hangx et al., 2010; Zhang et al., 2014). The increase of temperature will reduce the yield strength and peak strength of rock and make the rock become weak, essentially making the microscopic crystal plastic process such as dislocation movement and diffusion become active (Fossen, 2016). However, this view is based on certain confining pressure conditions, and only increasing the temperature at atmospheric pressure is not enough to make the rock become ductile (Paterson and Wong, 2005; Zhang, 2016). Figure 6 shows that the peak strength, residual strength and stress drop of mudstone after triaxial compression gradually decrease with the increase of temperature in the test temperature range of 25–160°C for the fifth group of samples, but the amplitude of the decrease and the overall shape of stress-strain curve have little change (Figure 5E). It shows that in the range of 160°C, the temperature does not have a decisive effect on the rock mechanical parameters of mudstone, and the change of formation temperature can only promote or inhibit the brittle and ductile transformation of rock to a certain extent, but the degree of influence is very limited. At present, the target stratum of petroliferaceous basin is generally located at 1–8 km, and the formation temperature is 40–200°C. Under this condition, without

FIGURE 4
Photos of mudstone samples after triaxial compression test under different conditions. **(A)** The Tugulu Group Formation in the southern margin of the Junggar Basin. **(B)** The Jidike Formation in Dongqiu anticline of the Kuche Depression in the Tarim Basin. **(C)** The Huangliu Formation in Ledong Area of the Yinggehai Basin. **(D)** The Huangliu Formation in Dongfang area of the Yinggehai Basin.

considering the confining pressure, the change of formation temperature has little influence on the mechanical properties of mudstone.

4.1.2 Confining pressure

With the increase of burial depth, the mechanical properties of the caprocks change from brittle stage to brittle-ductile stage, and finally enter the full ductile stage. The effect of burial depth on caprock mechanics is mainly reflected in the influence of temperature and confining pressure. By comparing the test results, it can be found that within the range of reservoir development depth, the effect of temperature on rock mechanics of caprock is limited (Figure 6), and confining pressure is the key factor affecting the mechanical properties and brittleness of mudstone (Figure 7). With the increase of confining pressure or burial depth, many rocks, such as limestone, dolomite, quartzite, salt

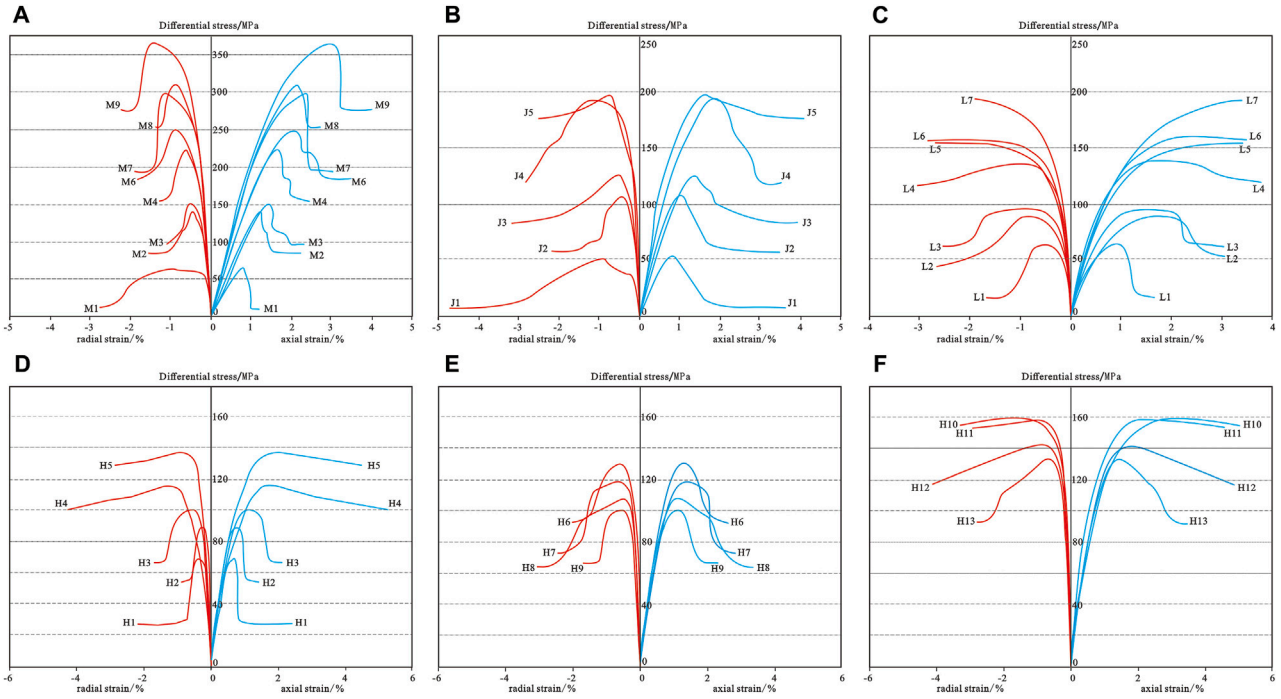

FIGURE 5
Stress-strain curves of mudstone samples under different conditions, **(A)** M1-M9 mudstone samples from Tugulu Formation in south Junggar Basin; **(B)** J1-J5 mudstone samples from Jidike Formation in of Dongqiu anticline, Kuqa Depression, Tarim Basin; **(C)** L1-L7 mudstone samples from Huangliu Formation in Ledong area, Yinggehai Basin; **(D)** H1-H5 mudstone samples from Huangliu Formation in Dongfang area, Yinggehai Basin; **(E)** H6-H9 mudstone samples from Huangliu Formation in Dongfang area, Yinggehai Basin; **(F)** H10-H13 mudstone samples from Huangliu Formation in Dongfang area, Yinggehai Basin.

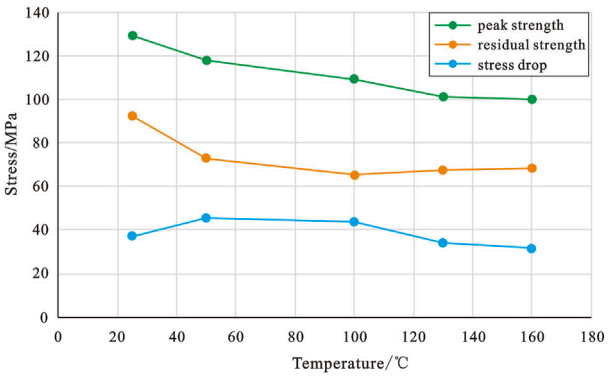

FIGURE 6
The relationship between rock mechanics and temperature of mudstones.

rock and gypsum, show similar brittle-ductile transformation characteristics, but the confining pressure of brittle-ductile transformation of rocks with different lithology is different.

Initially, Kármán confirmed the influence of confining pressure on rock brittle-ductile through his experimental study on Carrara marble, while Paterson revealed the nature of brittle and ductile transformation of rock with the increase of confining pressure through his experiment on Wombeyan marble. It can be seen from a large number of previous research results that the increase of confining pressure has three important effects on rock deformation: 1) With the increase of confining pressure, the stress variable before macroscopic rupture increases significantly, that is, from a small stress variable to produce macroscopic rupture to withstand a large change of dispersed stress variable; 2) the overall level of stress-strain curves is improved at higher confining pressures; 3) The degree of strain hardening is greater under higher confining pressure.

According to the stress-strain curves obtained by triaxial compression experiments of different mudstones (Figure 5), the stress variable before sample fractured increases significantly with the increase of confining pressure, and the peak strength and residual strength also increase correspondingly (Figure 7A, B), and the increase amplitude becomes slow after the confining pressure reaches 40 MPa, while the stress drop gradually decreases (Figure 7C). Theoretically, when the stress drop will be zero, the rock will enter the ductile deformation stage. In this experiment, the first group of samples (M1-M9) is always in the brittle stage, and the second group (J1-J5) and the fourth group (H1-H5) mudstone samples gradually change from brittle stage to brittle-ductile stage with the increase of confining pressure, and finally approach the ductile stage. The third group (L1-L7) mudstone samples have entered the ductile stage when the confining pressure exceeds 55 MPa. With the increase of confining pressure, the macroscopic deformation of the sample changes from tensile fracture to shear fracture, then to conjugate shear

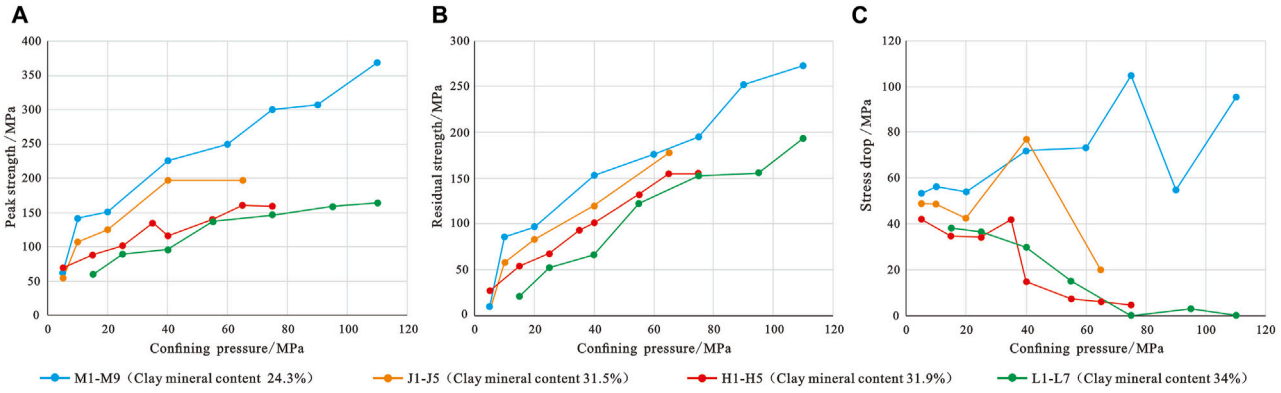

FIGURE 7
The relationship between rock mechanics and confining pressure of mudstones. **(A)** Peak strength; **(B)** Residual strength; **(C)** Stress drop.

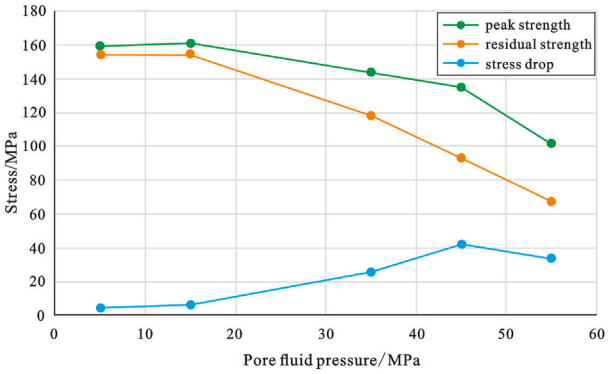

FIGURE 8
The relationship between rock mechanics and pore fluid pressure of mudstones.

fracture, and finally to ductile expansion (Figure 5). All these indicate that mudstone will transition to brittle stage and brittle-ductile stage with the increase of confining pressure.

4.1.3 Pore fluid pressure

In addition to confining pressure and temperature, the rock mechanical properties of mudstone are also affected by pore fluid pressure. Especially, in some basins, the deep layer often develops overpressure, which has a more significant impact on rock deformation. From the perspective of energy conservation, when a rock is under pressure, the pore fluid pressure inside the rock offsets part of the confining pressure. Therefore, the actual effective stress of rock should be the difference between confining pressure and pore fluid pressure. With the increase of pore fluid pressure, the effective stress decreases gradually, which inhibits the ductile deformation of rock and makes it more prone to brittle fracture of mudstone. It can be seen from the stress-strain curves of H3 and H10-H13 samples from Huangliu Formation of Yinggehai Basin that (Figure 5F), under the condition of constant lithology, confining pressure and temperature, with the increase of pore fluid pressure, the peak strength and residual strength of mudstone strain tend to decrease significantly (Figure 8), while the stress drop increases significantly. When the pore fluid pressure is less than 15 MPa, the stress-strain curve tends to flatten after reaching the peak strength, and the stress drop is close to zero, which is an obvious representation of rock entering ductile deformation. However, when the pore fluid pressure is greater than 45 MPa, the stress and strain curve falls significantly after reaching the peak strength, and the brittle fracture occurs. Therefore, due to the development of overpressure in the middle and deep layers of Yinggehai Basin, brittle fracture of rocks still occurs in spite of deep burial, which is of great significance for the study of the role of caprock on oil and gas preservation.

4.1.4 Lithology

At present, it is widely believed that the brittle and ductile of rock is related to the mineral composition of rock, and the critical transformation of the brittle ductile is mainly determined by the different responses of different minerals to temperature and pressure (Wang, 2021). The composition of mudstone minerals is complex, mainly composed of quartz, feldspar and clay minerals. Under the same temperature and pressure conditions, some minerals are brittle while others are ductile. Quartz deforms in a brittle mechanism at about 300°C–500°C and is about 10–12 km in crustal depth. At greater depths, creep and diffusion plastic deformation occur. Feldspar and olivine still showed brittle deformation at buried depths of 20–30–50 km, respectively (Fossen, 2016). Therefore, in the study of rock mechanics, it is generally believed that quartz is a brittle mineral, clay is a ductile mineral, and there is no clear definition on whether feldspar, carbonate minerals and pyrite are brittle minerals (Diao, 2013; Qin et al., 2016; He and Li, 2020; Liu et al., 2020; Wang et al., 2022).

The test samples in this study came from four blocks in three basins with similar rock and mineral composition, mainly consisting of quartz, feldspar, clay minerals, carbonate minerals and a small amount of other minerals (Table 2), but the content of each mineral is different to some extent. The results of the experiments showed that, under the condition of low confining pressure (confining pressure less than 5 MPa), the fracture peak strength of

mudstone samples does not differ much. With the increase of confining pressure, the peak intensity of Yinggehai basin samples is significantly lower than that of mudstone in the southern margin of Junggar Basin (Figure 7A). The peak strength is negatively correlated with the content of mudstone clay minerals, and the samples with high clay mineral content showed the characteristics of ductile deformation earlier. When confining pressure exceeds 60 MPa, the stress drop of Yinggehai Basin samples is close to zero (Figure 7C). It is worth noting that some previous studies believed that the increase of quartz content, makes the rock show more brittle properties, and the greater the peak strength of the rock fracture. However, the quartz content of the mudstone samples from Yinggehai Basin in this study is also slightly higher than that of other samples, but the peak strength is generally low. This may be because the quartz particles of mudstone in Yinggehai Basin have extremely fine particle size and are mainly suspended contact, and high clay content (Figure 3). Other studies have shown that the clay volume content is less than 15%, the particles support the rock, the clay has little influence on the elastic modulus, clay volume content is more than 35%, the main clay supports the rock, the average elastic modulus is controlled by the clay (Plumb, 1994; Wang, 2021). Although quartz content is high, it does not play the supporting role of rock skeleton. In the process of rock deformation, clay minerals dominate rock mechanical deformation.

In addition, some carbonate cementation was developed in mudstones of Yinggehai Basin, which were mainly calcite in terms of composition, while in Junggar Basin samples, besides calcite, there was 15% ankerite, which greatly improved the brittleness of rocks from the perspective of Young's modulus and Poisson's ratio, and thus resulted in a higher peak strength of rock fracture (Nelson, 2001; Diao, 2013). Therefore, when exploring the mechanical properties of rocks, we should not only analyze the brittleness degree of rocks from the mineral composition and content, but also pay attention to the spatial fabric and diagenesis of minerals.

4.2 Numerical simulation of the mudstone deformation characteristics under different geological conditions

Most of the previous studies on the mechanical properties of mudstones are based on mechanical experiments, but due to the difficulty of sampling the underground mudstone samples and the limited loading conditions of test equipment, most of the tests control a single variable to explore the change of rock mechanical experiments, but due to the rare number of mudstone samples and the limited loading conditions of test equipment, most of the experiments control a single variable to discuss the characteristic of rock mechanical properties. However, the real geological conditions are more complex. With the change of burial depth, confining pressure, temperature and pore pressure are constantly changing. Especially in some basins, abnormally high fluid pressure is developed in the middle and deep depths, such as Yinggehai Basin, one of the sources of this experimantal samples. Therefore, in order to reflect as much as possible the effects of confining pressure, temperature and pore fluid pressure on rock mechanics and rock deformation under real geological conditions, based on the triaxial compression test of rock mechanics in Yinggehai Basin, we obtained the mechanical parameters such as Young's modulus, Poisson's ratio, peak strength, residual strength, cohesion, internal friction angle and coefficient of internal friction of rocks under different temperature and confining pressure conditions, and constructed the numerical core by FLAC3D numerical simulation. By constantly adjusting the three-dimensional grid size and axial loading rate, the mechanical properties of the numerical core approximate the real test core properties, and finally determine the numerical core model. The same confining pressure conditions were applied on the FLAC3D software platform as in the laboratory experiment, and the results were compared with the experimental test results (Figure 9), the failure mode of the digital core is basically consistent with the failure mode of the experimental test sample, which fully verified the rationality of the numerical model established by FLAC3D software. On this basis, two sets of numerical simulations are carried out, which are under normal and overpressure systems respectively, so as to facilitate us better discuss the influence of fluid pressure on rock mechanics.

The first group simulates the rock under normal pressure system. The simulation results show that the characteristics of rock failure mode experienced the deformation process of a single high angle shear fracture, high angle conjugate shear fracture, low angle shear fracture and low angle conjugate fracture with increasing confining pressure and temperature (Figure 10).

When the buried depth is less than 2000 m, rock strength increases linearly with the buried depth, the strain is concentrated. At this stage, sample mainly develops the single shear fracture with high angle, and the peak strength is less than 100 MPa, showing brittle deformation. When the buried depth is between 2000 and 6,000 m and the peak strength is between 100–200 MPa, the strain gradually disperses from concentration, and the fracture mode evolves from single shear fracture to conjugate shear fracture, which is the transition stage of brittle and ductile deformation. When the burial depth is greater than 6,000 m, the peak strength is more than 200 MPa, the low-angle shear fractures are developed, strain showed a non-localized distribution, with insignificant rock destruction, and the local ductile expansion occurs. Only at higher temperature and pressure conditions can full ductile be achieved, which is difficult to achieve in real geological conditions (Figure 10).

The second group simulates the rocks under the overpressure system, and the fluid pressure magnitude refers to the formation pressure gradient of Yinggehai Basin. The simulation results show that (Figure 11), under the shallow burial condition, the strata generally do not develop abnormally high fluid pressure, and the rock deformation is consistent with the normal pressure system, and brittle shear fracture is developed. When the buried depth is greater than 2000 m, the rocks enter the brittle and ductile transition stage, and overpressure begins to appear in the formation. However, due to the small overpressure, the deformation of the rocks is not significantly affected, and the rock is mainly subjected to tensile shear fracture, forming conjugate fractures. When the buried depth of the local layer exceeds 3,000 m and the formation pressure coefficient exceeds 1.5, compared with the first group of simulation results, the rock strength no longer increases

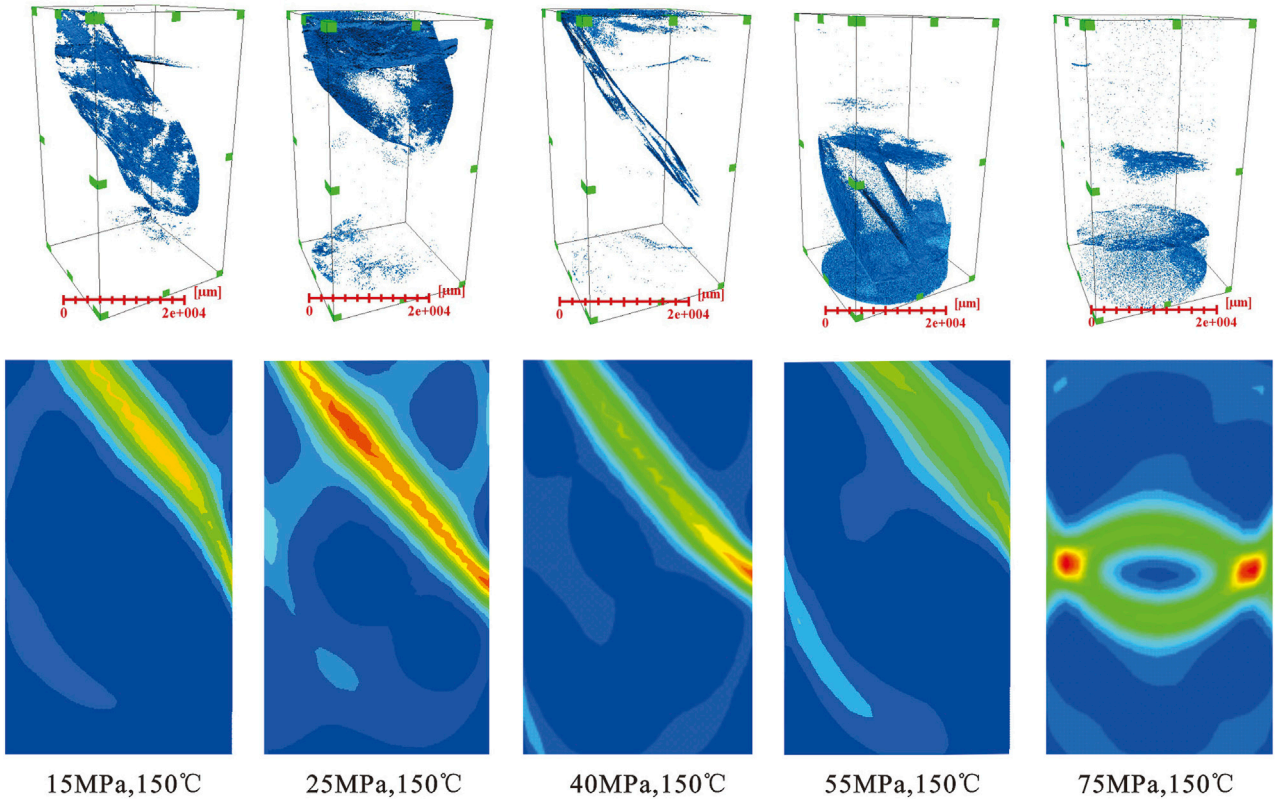

FIGURE 9
CT scanning of mudstone samples after triaxial compression test and numerical simulation under corresponding test conditions.

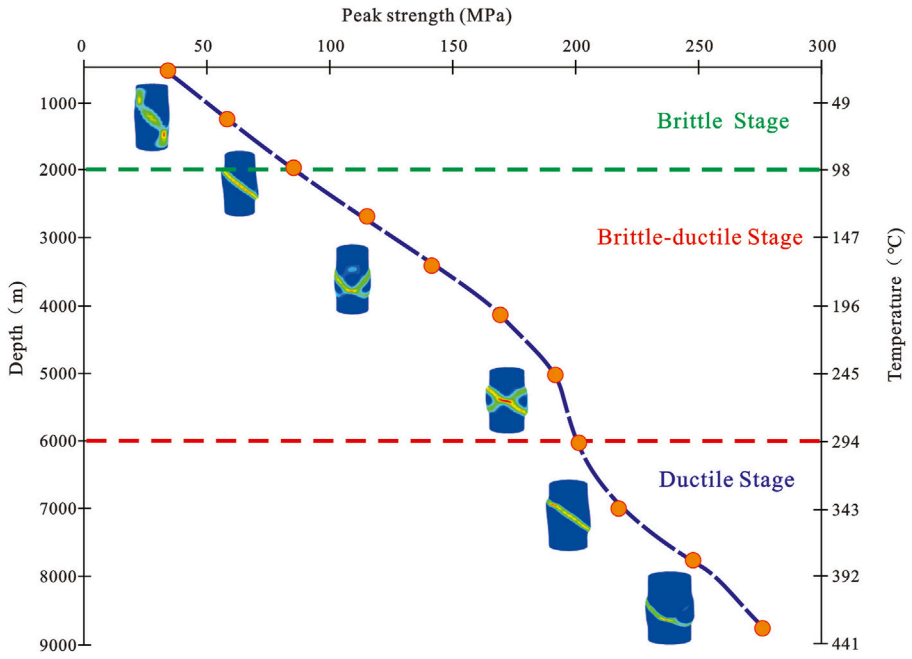

FIGURE10
Evolution of mudstone fracture deformation with buried depth under normal pressure system.

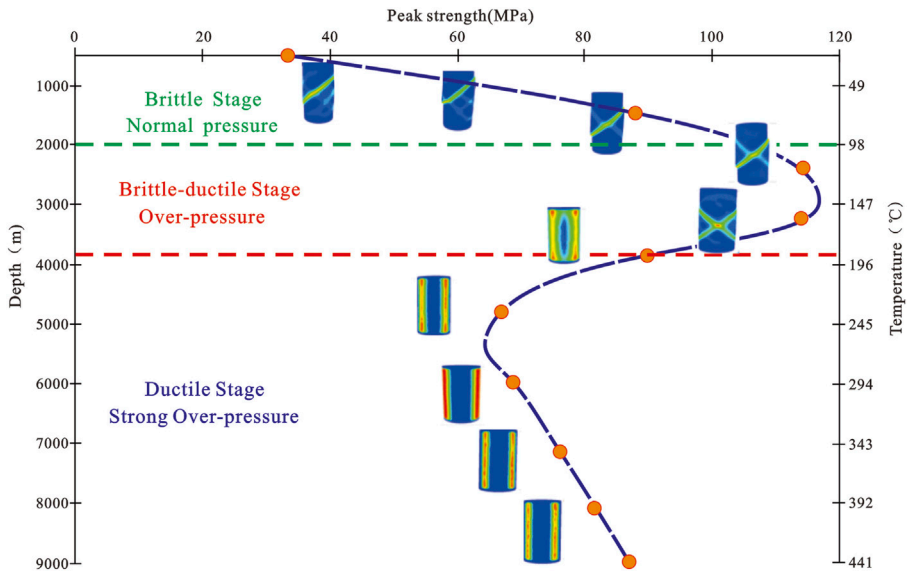

FIGURE 11
Evolution of mudstone fracture deformation with buried depth under overpressure system.

continuously, but begins to decrease gradually. When the buried depth increases to 3,900 m and the formation pressure coefficient reaches 2.0, under the effect of strong overpressure, the mechanics deformation of rocks begin to reverse. Instead of transitioning to ductile stage, the rock re-enters the brittle stage. The brittle fracture of the rock develops obviously, but the fracture property changes from shear fracture to tensile fracture. Digital core can clearly see the stress concentration development of tensile fracture.

The numerical simulation under normal pressure system is almost consistent with our conventional understanding, and can be mutually verified by a large number of rock mechanics experiments (Fu et al., 2015; Wang et al., 2019; Wu et al., 2022). In the overpressured basin, especially in Yinggehai Basin, many published papers have mentioned that the deep overpressured layer is affected by fluid pressure and the coupling of pressure and stress, which makes the formation more prone to tensile fracture, especially in the deep overpressured layer where shear fracture should occur according to the classical model (Hao et al., 2015; Jia et al., 2021). However, these studies are almost all based on the work of theoretical calculation, and the numerical simulation results just confirm the conclusion. This tension rupture can lead to cap rupture and oil and gas leakage, controlling and affecting the migration, accumulation and distribution of oil and gas in the overpressure basin at multiple levels.

4.3 The influence of rock mechanical properties and brittle-ductile stage on caprock integrity

The main objective of studying the mechanical properties of mudstone is to evaluate the critical conditions for the transition from brittle to ductile of caprocks. Because the sealing ability of the caprocks in most oil and gas fields does not have the leakage risk, the real cause of oil and gas escape is the destruction of cap integrity (Fu et al., 2018; Jia, 2018). However, the rupture characteristics of different brittle and ductile caprocks are different, which need to be evaluated by targeted methods (Fu et al., 2018; Jia, 2018; Wu, 2020).

Based on the results of laboratory experiments and numerical simulation, under the condition of shallow burial, that is, when the formation temperature and confining pressure are low, the caprock is often in the brittle stage. At the initial stage of stress and deformation, a large number of shear fractures are formed inside the rock. With the increase of deformation strength, the fracture density gradually increases and the fracture length constantly expands. Finally, these fractures are gradually connected and formed fault. Field observation has proved that brittle caprock rupture will generally form a large penetrated fault, and the damage degree of such fautl to caprock is jointly affected by caprock thickness and fault distance. Therefore, the difference between caprock thickness and fault distance is defined as the juxtaposition thickness quantitatively represent the degree of damage of the fault to the caprock (Lv et al., 2014). At present, the statistics of oil and water distribution laws in multiple basins show that there are critical value of juxtaposition thickness in brittle stage (Sun et al., 2013; Lv et al., 2014; Fu et al., 2015), the weaker the fault damage to the caprock is weaker with the larger of the value and the stronger of the caprock sealing ability.

With the increase of burial depth, mudstone deformation gradually shows the component of ductile after the caprock enters the brittle-ductile transition stage. The larger the buried depth, the stronger the rheological feature, until it enters the full ductile stage. In the brittle-ductile stage, conjugate shear fracture is developed in rocks, which is no longer a macroscopically penetrated fault, but a smear fault. The phenomenon of smearing has been widely confirmed in the field outcrops and physical simulation tests (Aydin and Eyal, 2002; Takahashi, 2002; Doughty, 2003; Koledoye

et al., 2003; Fu et al., 2015; Wang et al., 2022; Wang et al., 2022). As long as the smear maintains continuity, the fault keeps sealing ability in vertically. Most scholars believe that the smear-continuity of mudstone is controlled by the ratio of fault distance to mudstone thickness, namely, Shale smear factor (SSF). There are obvious differences in sealing critical SSF among different lithologies, the SSF smaller than the critical value of mudstone is vertically sealed.

The caprock in the ductile stage has the characteristics of ductile flow, but due to the high required temperature and confining pressure, it is difficult to achieve in real geological conditions. Except for some known gypsum rock and salt rock caprock, no ductile mudstone rock caprock has been found in the depth range of oil and gas distribution at present.

It should be emphasized that if the formation develop overpressure, it will inhibit the brittleness transformation process of rock. When it reaches a certain extent, and even make the rock by brittle-ductile transition stage reverse conversion to brittle stage, and the fracture mode will also change from conjugate fracture to almost vertical tensile fracture, which has been confirmed by the numerical simulation above. In the world, there are about 180 basins with abnormal pressure, most of which are overpressure basins. Overpressure may lead to tensile fracture of caprock, and then lead to oil and gas loss. This phenomenon has been found in Yinggehai Basin. Therefore, in the actual evaluation of caprock, the brittle and ductile of caprock cannot be evaluated only by the change of buried depth or confining pressure, especially in the overpressure developed caprock, the influence of pore fluid pressure on the brittle and ductile transformation of caprock should be considered. To correctly evaluate the brittle and ductile stage of caprock and to specify the fracture mode of caprock is the key to evaluate the integrity of caprock.

5 Conclusion

The rock mechanics triaxial compression test was carried out with mudstone samples from three basins, and different test conditions of confining pressure, temperature and pore fluid pressure were set up respectively. The mechanical parameters of mudstone were extracted from the test in Yinggehai Basin, and established a numerical model of mudstone, after verifying the reliability of the model, the rock deformation under normal pressure system and overpressure system was simulated. The influence of different geological factors on the mechanical properties and deformation characteristics of mudstone is analyzed by combining the test results and numerical simulation results. The following conclusions are obtained:

(1) The mechanical properties of mudstone are most significantly affected by confining pressure. With the increase of confining pressure, mudstone gradually changes from brittles stage to brittle-ductile stage, and ductile stage, and the fracture mode changes from single shear fracture to conjugate shear fracture, and finally to ductile expansion. Compared with confining pressure, temperature has limited influence on caprock at current hydrocarbon enrichment depth.
(2) The results of this experiments show that the brittleness of mudstone is not significantly correlated with the content of quartz mineral, but is negatively correlated with the content of clay mineral. The main reason is that the quartz particle size is fine, the contact between particles is suspended, and the matrix is mainly clay minerals.
(3) The results of the numerical simulation show that, pore fluid pressure has an obvious inhibition effect on the brittle and ductile transformation process of rock. With the increase of the overpressure to a certain extent, the mudstone no longer occurs the classic brittle ductile transformation, but returns from the brittle-ductile stage to the brittle stage, and the fracture mode changes from shear fracture to tensile fracture.

Data availability statement

The original contributions presented in the study are included in the article/Supplementary Material, further inquiries can be directed to the corresponding author.

Author contributions

RJ: conceptualization, methodology, writing—original draft, visualization. XF: writing—review and editing, investigation, supervision. YJ: formal analysis, investigation, resources. TW: validation, formal analysis, visualization. SW: conceptualization, methodology, formal analysis, HC: data curation, visualization. All authors contributed to the article and approved the submitted version.

Funding

This study is supported by the National Natural Science Foundation of China (42002152); the Natural Science Foundation of Heilongjiang Province (LH 2021D006); the China Postdoctoral Science Foundation Project (2022MD723758); the Postdoctoral Project of Heilongjiang Province (LBH-Z22096), Academician Innovation Platform Scientific Research Project of Hainan Province (YSPTZX202301).

Conflict of interest

Author HC was employed by the company Daqing Yusulin Oilfield Development Co., Ltd.

The remaining authors declare that the research was conducted in the absence of any commercial or financial relationships that could be construed as a potential conflict of interest.

Publisher's note

References

Aydin, A., and Eyal, Y. (2002). Anatomy of a normal fault with shale smear: Implications for fault seal. *AAPG Bull.* 86, 1367–1381. doi:10.1306/61EEDC9C-173E-11D7-8645000102C1865D

Basu, A., Mishra, D., and Roychowdhury, K. (2013). Rock failure modes under uniaxial compression, Brazilian, and point load tests. *Bull. Eng. Geol. Environ.* 72 (3-4), 457–475. doi:10.1007/s10064-013-0505-4

Brantut, N., Schubnel, A., and Guéguen, Y. (2011). Damage and rupture dynamics at the brittle-ductile transition: The case of gypsum. *J. Geophys. Res. Solid Earth* 116 (B1), B01404. doi:10.1029/2010jb007675

Chen, W., Wan, W., Zhao, Y., and Peng, W. (2020). Experimental study of the crack predominance of rock-like material containing parallel double fissures under uniaxial compression. *Sustainability* 12 (12), 5188. doi:10.3390/su12125188

Corcoran, D. V., and Dore, A. G. (2002). Top seal assessment in exhumed basin settings-some insights from Atlantic Margin and borderland basins. *NPF Spec. Publ.* 11 (02), 89–107. doi:10.1016/S0928-8937(02)80009

Dewhurst, D. N., Jones, R. M., and Raven, M. D. (2002). Microstructural and petrophysical characterization of muderong shale: Application to top seal risking. *Pet. Geosci.* 8 (4), 371–383. doi:10.1144/petgeo.8.4.371

Diao, H. Y. (2013). Rock mechanical properties and brittleness evaluation of shale reservoir. *Acta Petrol. Sin.* 29 (9), 3300–3306. doi:10.1086/671395

Doughty, P. T. (2003). Clay smear seals and fault sealing potential of an exhumed growth fault, Rio Grande rift, New Mexico. *AAPG Bull.* 87 (3), 427–444. doi:10.1306/10010201130

Downey, M. W. (1984). Evaluating seals for hydrocarbon accumulations. *AAPG Bull.* 68 (11), 1752–1763.

Faerseth, R. B., Johnsen, E., and Sperrevik, S. (2007). Methodology for risking fault seal capacity: Implications of fault zone architecture. *AAPG Bull.* 91 (9), 1231–1246. doi:10.1306/03080706051

Fossen, H. (2016). *Structural geology*. United States: Cambridge University Press.

Fu, G., Liu, B., and Lv, Y. F. (2008). Comprehensive evaluation method for sealing ability of mudstone caprock to gas in each phase. *Lithol. Reserv.* 20 (1), 21–26. doi:10.3969/j.issn.1673-8926.2008.01.004

Fu, G., Wang, H. R., and Hu, X. L. (2015a). Prediction method and application of caprock faulted-contact thickness lower limit for oil-gas sealing in fault zone. *J. China Univ. Petroleum* 39 (3), 30–37. doi:10.3969/j.issn.1673-5005.2015.03.004

Fu, X. F., Jia, R., and Wang, H. X. (2015b). Quantitative evaluation on the fault-caprock sealing capacity of Dabei-kelasu structural belt in Kuqa depression, Tarim basin, NW China. *Petroleum Explor. Dev.* 42 (3), 300–309. doi:10.1016/S1876-3804(15)30023-9

Fu, X. F., Wu, T., and Lv, Y. F. (2018). Research status and development trend of the reservoir caprock sealing properties. *Oil Gas Geol.* 39 (3), 454–471. doi:10.11743/ogg20180304

Fuenkajorn, K., Sriapai, T., and Samsri, P. (2012). Effects of loading rate on strength and deformability of Maha Sarakham salt. *Eng. Geol.* 135, 10–23. doi:10.1016/j.enggeo.2012.02.012

Gao, X., Yang, C., and Wu, W. (2005). Experimental studies on temperature effect of mechanical properties of rock salt. *Rock Soil Mech.* 26 (11), 1775–1778. doi:10.1080/02533839.2005.9671036

Grunau, H. R. (1987). A worldwide look at the cap-rock problem. *J. Petroleum Geol.* 10 (3), 245–265. doi:10.1111/j.1747-5457.1987.tb00945.x

Handin, J., Hager, R. V., and Friedman, M. (1963). Experimental deformation of sedimentary rocks under confining pressure: Pore pressure tests. *AAPG Bull.* 47 (5), 717–755.

Hangx, S., Spiers, C., and Peach, C. (2010). Mechanical behavior of anhydrite caprock and implications for CO_2 sealing capacity. *J. Geophys. Res. Atmos.* 115 (B7), 074022–B8139. doi:10.1029/2009jb006954

Hao, F., Liu, J., and Zou, H. (2015). Mechanisms of natural gas accumulation and leakage in the overpressured sequences in the Yinggehai and Qiongdongnan basins, offshore South China Sea. *Earth Sci. Front.* 22 (1), 169–180. doi:10.13745/j.esf.2015.01.014

He, X., and Li, Q. (2020). Quantitative definition and evaluation of brittle minerals in shale based on statistics: Taking shale of wufeng -longmaxi Formation in sichuan Basin and its peripheral area as an example. *J. Xi'an Shiyou Univ. Nat. Sci. Ed.* 35 (2), 42–49. doi:10.3969/j.issn.1673-064X.2020.02.006

Heuze, F. (1983). High-temperature mechanical, physical and thermal properties of granitic rocks-a review. *Int J Rock Mech Min Sci Geo Mech Abstr* 20 (1), 3–10. doi:10.1016/0148-9062(83)91609-1

Ingram, G. M., Urai, J. L., and Naylor, M. A. (1997). Sealing processes and top seal assessment. *Nor. Pet. Soc. Spec. Publ.* 7, 165–174.

Ingram, G. M., and Urai, J. L. (1999). Top-seal leakage through faults and fractures: The role of mudrock properties. *Geol. Soc. Lond. Spec. Publ.* 158 (1), 125–135. doi:10.1144/gsl.sp.1999.158.01.10

Jia, R., Fan, C., Liu, B., Fu, X., and Jin, Y. (2021). Analysis of natural hydraulic fracture risk of mudstone cap rocks in XD block of central depression in Yinggehai Basin, south China Sea. *Energies* 14 (14), 4085. doi:10.3390/en14144085

Jia, R. (2018). *The integrity of caprocks and gas accumulation in Yingqiong Basin*. Daqing: Northeast Petroleum University.

Jin, Z., Yuan, Y., Liu, Q., and Wo, Y. (2013). Controls of Late Jurassic-Early Cretaceous tectonic event on source rocks and seals in marine sequences, South China. *Sci. China Earth Sci.* 56 (2), 228–239. doi:10.1007/s11430-012-4494-0

Koledoye, B. A., Aydin, A., and May, E. (2003). A new process-based methodology for analysis of shale smear along normal faults in the Niger Delta. *AAPG Bull.* 87 (3), 445–463. doi:10.1306/08010200131

Li, H., Fan, C. W., and Jiang, Z. X. (2022). Natural fractures in low-PermeabilitySandstone reservoirs in the LD-A HPHT gas field, Yinggehai Basin: Implications for hydrocarbonb exploration and development. *Front. Earth Sci.* 10, 934097. doi:10.3389/feart.2022.934097

Li, S. J., Jin, Z. J., and Yuan, Y. S. (2016). Triaxial stress experiment of mudstone under simulated geological conditions and its petroleum significance. *Oil Gas Geol.* 37 (4), 598–605. doi:10.11743/ogg20160418

Liu, B., Wang, S., Ke, X., Fu, X., Liu, X., Bai, Y., et al. (2020). Mechanical characteristics and factors controlling brittleness of organic-rich continental shales. *J. Petroleum Sci. Eng.* 194, 107464. doi:10.1016/j.petrol.2020.107464

Lu, X. S., Liu, S. B., and Tian, H. (2021). An evaluation method for the integrity of mudstone caprock in deep anticlinal traps and its application: A case study of the sinian gas reservoirs in the central sichuan basin. *Acta Pet. Sin.* 42 (4), 415–427. doi:10.7623/syxb202104001

Lv, Y. F., Fu, G., and Gao, D. L. (1996). *Study on the cap rock of reservoir*. Beijing: Petroleum Industry Press.

Lv, Y. F., Xu, C. L., and Fu, G. (2014). Oil-controlling models of caprock-fault combination and prediction of favorable horizons for hydrocarbon accumulation in middle-shallow sequences of Nanpu sag. *Oil Gas Geol.* 35 (1), 86–97. doi:10.11743/ogg20140111

Ma, D., Duan, H., Zhang, J., Liu, X., and Li, Z. (2022). Numerical simulation of water–silt inrush hazard of fault rock: A three-phase flow model. *Rock Mech. Rock Eng.* 55, 5163–5182. doi:10.1007/s00603-022-02878-9

Ma, D., Li, Q., Cai, K., Zhang, J. X., Li, Z. H., Hou, W. T., et al. (2023). Understanding water inrush hazard of weak geological structure in deep mine engineering: A seepage-induced erosion model considering tortuosity. *J. Central South Univ.* 30 (2), 517–529. doi:10.1007/s11771-023-5261-4

Mildren, S. D., Hillis, R. R., and Dewhurst, D. N. (2005). "Fast: A new technique for geomechanical assessment of the risk of reactivation-related breach of fault seals," in *AAPG hedberg series* (Barossa Valley, South Australia: Evaluating fault and cap rock seals), 73–85.

Nelson, R. A. (2001). *Geologic and analysis of naturally fractured reservoirs*. Geologic Analysis of Naturally Fractured Reservoirs, 323–332.

Nygård, R., Gutierrez, M., Bratli, R. K., and Høeg, K. (2006). Brittle-ductile transition, shear failure and leakage in shales and mudrocks. *Mar. Petroleum Geol.* 23 (2), 201–212. doi:10.1016/j.marpetgeo.2005.10.001

Ovcharenko, A. V., Ermakov, B. V., Myatchin, K. M., and Shlezinger, A. E. (2007). Caprocks in hydrocarbon fields. *Lithology Mineral Resour.* 42 (2), 180–191. doi:10.1134/s0024490207020058

Paterson, M. S. (1958). Experimental deformation and faulting in wombeyan marble. *Geol. Soc. Am. Bull.* 69 (4), 465. doi:10.1130/0016-7606(1958)69[465:edafiw]2.0.co;2

Paterson, M. S., and Wong, T. (2005). *Experimental rock deformation-the brittle field*. Springer Science & Business Media.

Plumb, R. (1994). "Influence of composition and texture on the failure properties of clastic rocks," in *SPE rock mechanics in Petroleum engineering* (Delft, Netherlands: SPE), 13–20.

Qin, X. Y., Wang, Z. L., and Yu, H. Y. (2016). A new shale brittleness evaluation method based on rock physics and mineral composition. *Nat. Gas. Geosci.* 27 (10), 1924–1932. doi:10.11764/j.issn.1672-1926.2016.10.1924

Sun, Y. H., Zhao, B., and Dong, Y. X. (2013). Control of faults on hydrocarbon migration and accumulation in the Nanpu Sag. *Oil Gas Geol.* 34 (4), 540–549. doi:10.11743/ogg20130417

Takahashi, M. (2002). Permeability change during experimental fault smearing. *J. Geophys. Res.* 108, 2234. doi:10.1029/2002jb001984

Tian, X., Zhuo, Q., and Zhang, J. (2017). Sealing capacity of the Tugulu Group and its significance for hydrocarbon accumulation in the lower play in the southern Junggar Basin, northwest China. *Oil Gas Geol.* 38 (2), 334–344.

Wang, H., Fu, X., Fan, M., Wang, S., Meng, L., and Du, W. (2022a). Fault growth and linkage: Implications for trap integrity in the qi'nan area of the huanghua depression in bohai bay basin, China. *Mar. Petroleum Geol.* 145, 105875. doi:10.1016/j.marpetgeo.2022.105875

Wang, H., Wu, T., Fu, X., Liu, B., Wang, S., Jia, R., et al. (2019). Quantitative determination of the brittle-ductile transition characteristics of caprocks and its

geological significance in the Kuqa depression, Tarim Basin, Western China. Journal of *Petroleum Science and Engineering*. *J. Pet. Sci. Eng.* 173, 492–500. doi:10.1016/j.petrol.2018.10.042

Wang, S., Liu, K., Wang, H., and Chen, M. (2022b). Growth and linkage of normal faults experiencing multiple non-coaxial extension: A case from the qikou sag, bohai bay basin, east China. *Basin Res.* 34 (2), 748–770. doi:10.1111/bre.12639

Wang, S. (2021). *Study on the main controlling factors of brittleness and compressibility classification evaluation for tight reservoirs*. Daqing: Northeast Petroleum University.

Wu, T., Fu, X., Wang, H., Lu, M., Meng, L., and Gong, L. (2022). Mechanism and continuity of gypsum smears in the East Qiulitage anticline, Kuqa foreland basin, China. *AAPG Bull.* 106 (8), 1605–1623. doi:10.1306/02072219057

Wu, T. (2020). *Study on the dynamic evolution of sealing capacity of mudstone and gypsum caprocks*. Daqing: Northeast Petroleum University.

Xie, Y. (2009). *Sequence stratigraphic analysis and hydrocarbon accumulation models in tectonically active basins: Case study on the Yinggehai Basin*. Beijing: Geological Publishing House.

Xie, Y., Zhang, Y., Li, X., Wu, E., Veasley, C., and Dade, C. (2012). Economic burden and quality of life of vulvodynia in the United States. *Acta Pet. Sin.* 33 (7), 601–608. doi:10.1185/03007995.2012.666963

Yu, w., Li, K., Liu, Z., An, B., Wang, P., and Wu, H. (2021). Mechanical characteristics and deformation control of surrounding rock in weakly cemented siltstone. *Environ. Earth Sci.* 80 (9), 337. doi:10.1007/s12665-021-09626-2

Zhang, C. (2016). The stress–strain–permeability behaviour of clay rock during damage and recompaction. *J. Rock Mech. Geotechnical Eng.* 8 (1), 16–26. doi:10.1016/j.jrmge.2015.10.001

Zhang, C., Xu, X., Zhang, Y., and Zhang, Y. (2014). Seasonal and diurnal variations of atmospheric peroxyacetyl nitrate, peroxypropionyl nitrate, and carbon tetrachloride in Beijing. *J. Inf. Technol. Civ. Eng. Archit.* 6 (2), 65–74. doi:10.1016/s1001-0742(13)60382-4

Zhao, Y., Wang, Y., Wang, W., Tang, L., Liu, Q., and Cheng, G. (2019). Modeling of rheological fracture behavior of rock cracks subjected to hydraulic pressure and far field stresses. *Theor. Appl. Fract. Mech.* 101, 59–66. doi:10.1016/j.tafmec.2019.01.026

Zhao, Y., Zhang, C., Wang, Y., and Lin, H. (2021). Shear-related roughness classification and strength model of natural rock joint based on fuzzy comprehensive evaluation. *Int. J. Rock Mech. Min. Sci.* 137, 104550. doi:10.1016/j.ijrmms.2020.104550

Zhao, Y., Zhang, C., Wang, Y., Liu, Q., Tang, L., and Cheng, G. (2020). Experimental study on shear behavior and a revised shear strength model for infilled rock joints. *Int. J. Geomechanics* 20 (9), 04020141. doi:10.1061/(asce)gm.1943-5622.0001781